Safe Current Injection Strategies for a STATCOM under Asymmetrical Grid Faults

Pedro Rodriguez
IEEE Senior Member

Gustavo Medeiros
IEEE Student Member

Alvaro Luna
IEEE Student Member

Marcelo C. Cavalcanti
IEEE Member

Remus Teodorescu
IEEE Senior Member

Technical University of Catalonia
C/Colom nº1, Terrassa 08222
prodriguez@ee.upc.edu

***Abstract*- This paper explores different strategies to set the reference current of a STATCOM under unbalanced grid voltage conditions and determines the maximum deliverable reactive power in each case to guarantee the injected current is permanently within the STATCOM secure operation limits. The paper presents a comprehensive derivation of the proposed STATCOM control strategies to set the reactive current reference under unbalanced grid faults, together with an extensive evaluation using simulation and experimental results from a low-scale laboratory setup in order to verify and validate the dynamic performance achieved by the proposed reactive current limiting algorithms.**

***Index Terms*— Current Control, Current limiters, Reactive Power, Reactive Power Control**

I. INTRODUCTION

Power electronics systems offer new ways for controlling reactive power in both high-voltage transmissions and low-voltage distribution systems. Reactive power control allows both regulating the voltage level in transmission systems, for maintaining a stable operation of the power system, and compensating particular loads, to improve the supply and demand quality in such loads [1].

Last advances in power semiconductors have aroused the Static Synchronous Compensator (STATCOM) as an effective solution that overcomes the limitations of the Static Var Compensators (SVC) in medium-voltage distribution systems. The STATCOM generally uses a voltage source converter (VSC) to accurately regulate the reactive current injected into the grid terminal, which allows injecting full rated current almost independently of the system voltage level [2]. Moreover, the STATCOM offers an excellent dynamic performance in controlling reactive power [3]. All these features, plus high efficiency and small footprint, make the STATCOM a very suitable solution to increase the operational efficiency and stability of power systems [4], to mitigate the effects caused on the grid by fluctuating loads as arc furnaces [5], to achieve fast and accurate voltage regulation at critical loads [6] and to satisfy reactive current requirements regarding the grid connection of distributed generators [7].

The STATCOM's manufacturers have gained a remarkable share in the market of electrical equipments for wind parks in the last years. This is due to the fact that the STATCOM has demonstrated to be a powerful solution to allow certain wind turbines (WT) to agree with the strict grid connection rules imposed by the transmission system operator (TSO) in countries with large-scale integration of wind power [8]-[10]. The effectiveness of the STATCOM in improving both the transient response and the low voltage ride through capability of wind farms based on IG and DFIG has been reported in [11]. In all these works, it is demonstrated that the STATCOM action enhances the performance of the wind farm when affected by balanced voltage sags. These studies match to that stated in the grid code requirements, since almost all the grid codes in force set requirements considering balanced voltage conditions, and just short comments are made regarding wind farm performance during unbalanced faults [8][10]. In practice however, more than 90% of the grid faults result in unbalanced voltages sags.

Even very short-time unbalanced voltages sags are extremely hazardous for a STATCOM since they might trigger the power converter shutdown as a consequence of reaching either the maximum instantaneous output overcurrent limit or the maximum instantaneous overvoltage/undervoltage limit on the dc-bus. Obviously, a sudden disconnection of the STATCOM would lead the controlled power system into a very risky state.

A stand-by operation mode to protect the STATCOM under unbalanced grid voltages was addressed in [12]. In [13], it was demonstrated that a properly controlled STATCOM might independently compensate the positive- and negative-sequence components of unbalanced voltage sags. Recently in [14], three STATCOM control schemes were evaluated under unbalanced voltages by using a steady-

state analysis, being concluded that, for a given compensation performance, the lowest STATCOM rating is achieved when it works as a voltage controlled current source exclusively injecting negative sequence current into the grid. Even though the need of limiting the STATCOM output current to ride through transient faults it is pointed out in [13], there is not any detailed study about this crucial matter in the literature.

This paper studies different strategies for injecting reactive current during unbalanced grid faults and finds mathematical expressions to set the limit of the reactive power delivered by the STATCOM during such transient unbalanced grid conditions in order to guarantee its safe operation. In this respect, a detailed analysis of the reactive current vector locus is conducted for each of the proposed control strategies and the reactive power capability of the STATCOM under generic unbalanced grid conditions is evaluated.

II. Strategies for Reactive Power Delivering

As shown in [30], some strategies to deliver reactive power into the grid under unbalanced conditions result in injecting nonsinusoidal currents, which imposes high dynamic requirements to the current controller, increases the voltage distortion at the point of common coupling and might originates grid resonances. In this section, those other reactive control strategies injecting sinusoidal currents into the grid are reviewed and commented.

According to the instantaneous power theory, the instantaneous reactive power q delivered by a reactive current vector $\mathbf{i}_q$ interacting generic voltage vector $\mathbf{v}$, is given by:

$$q = \left| \mathbf{v} \times \mathbf{i}_q \right|, \tag{1}$$

where the sign $\times$ denotes a cross product. The instantaneous reactive power can be also calculated by the dot product:

$$q = \mathbf{v}_\perp \cdot \mathbf{i}_q, \tag{2}$$

where $\mathbf{v}_\perp$ is an ortogonal (90-degrees leaded) version of the original grid voltage vector $\mathbf{v}$. Since the positive- and negative-sequence components of the reactive current injected by the STATCOM must be properly controlled, it will assumed from here on that this current vector consists of a positive- and a negative sequence components, i.e., $\mathbf{i}_q = \mathbf{i}_q^+ + \mathbf{i}_q^-$. If this unbalanced current vector is injected into an unbalanced grid with $\mathbf{v} = \mathbf{v}^+ + \mathbf{v}^-$, therefore the instantaneous reactive power will be given by:

$$q = \mathbf{v}_\perp^+ \cdot \mathbf{i}_q^+ + \mathbf{v}_\perp^- \cdot \mathbf{i}_q^- + \mathbf{v}_\perp^+ \cdot \mathbf{i}_q^- + \mathbf{v}_\perp^- \cdot \mathbf{i}_q^+ . \tag{3}$$

.

A. Positive-Negative-Sequence Compensation (PNSC)

the *PNSC* strategy, the reactive power delivered to the grid results from the interaction between voltages and currents with the same sequence. Moreover, it is imposed as a condition that oscillations in the reactive power resulting from the interaction of voltages and currents with different sequences should be mutually cancelled, i.e.,

$$Q = \mathbf{v}_\perp^+ \mathbf{i}_q^{*+} + \mathbf{v}_\perp^- \mathbf{i}_q^{*-} \quad ; \quad 0 = \mathbf{v}_\perp^+ \mathbf{i}_q^{*-} + \mathbf{v}_\perp^- \mathbf{i}_q^{*+} . \tag{4}$$

This strategy gives rise to sinusoidal current waveforms even under unbalanced grid voltage conditions, being the reference currents calculated as follow:

$$\mathbf{i}_\mathbf{q}^* = \mathbf{i}_\mathbf{q}^{*+} + \mathbf{i}_\mathbf{q}^{*-} = b^\pm \left(\mathbf{v}_\perp^+ - \mathbf{v}_\perp^- \right), \qquad b^\pm = \frac{Q}{|\,\mathbf{v}_\perp^+\,|^2 - |\,\mathbf{v}_\perp^-\,|^2}. \tag{5}$$

In this strategy, the interaction between voltage and current components with different sequences does not deliver any net active power but gives rise to power oscillations at twice the fundamental utility frequency, i.e.,

$$p = \mathbf{v} \cdot \mathbf{i}_\mathbf{q}^* = \underbrace{\mathbf{v}^+ \cdot \mathbf{i}_\mathbf{q}^{*+} + \mathbf{v}^- \cdot \mathbf{i}_\mathbf{q}^{*-}}_{0} + \underbrace{\mathbf{v}^+ \cdot \mathbf{i}_\mathbf{q}^{*-} + \mathbf{v}^- \cdot \mathbf{i}_\mathbf{q}^{*+}}_{\tilde{p}}. \tag{6}$$

B.- Average Active-Reactive Control (AARC)

In the *AARC* strategy, the reference reactive current vector $\mathbf{i}_q^*$ is monotonously proportional to the in-quadrature voltage vector $\mathbf{v}_\perp$. That is,

$$\mathbf{i}_\mathbf{q}^* = \mathbf{i}_\mathbf{q}^{*+} + \mathbf{i}_\mathbf{q}^{*-} = B\, \mathbf{v}_\perp \quad ; \quad B = \frac{Q}{V_\Sigma^2}. \tag{7}$$

In (7), the susceptance B is a constant since it is calculated from the collective rms value of the grid voltage, which is defined by:

$$V_\Sigma = \sqrt{\frac{1}{T}\int_0^T |\,\mathbf{v}\,|^2\, dt} = \sqrt{|\,\mathbf{v}^+\,|^2 + |\,\mathbf{v}^-\,|^2}\,. \tag{8}$$

The reference current vector of (7) has the same direction as the in-quadrature voltage vector $\mathbf{v}_\perp$, so giving rise to no active power. However the reactive power consists of an average value equal Q plus an oscillating term at twice the grid frequency, that is:

$$q = \mathbf{v}_\perp \cdot \mathbf{i}_q^* = \frac{|\,\mathbf{v}\,|^2}{V_\Sigma^2} Q = Q + \tilde{q} = Q\left[1 + \frac{2\,|\mathbf{v}^+|\,|\mathbf{v}^-|}{|\mathbf{v}^+|^2 + |\mathbf{v}^-|^2} \cos(2\omega t + \phi^+ - \phi^-) \right], \tag{9}$$

where ϕ^+ and ϕ^- are the phase-angles of the positive- and negative-sequence voltage vector components $\mathbf{v}^+$ and $\mathbf{v}^-$, respectively.

C.- Balanced Positive-Sequence Control (BPSC)

In the *BPSC* strategy, the injected reactive currents are perfectly balanced and monotonously proportional to the in-quadrature positive-sequence voltage vector as the averaged positive-sequence susceptance B^+ is a constant as well, i.e.,

$$\mathbf{i}_{\mathbf{q}}^{*} = \mathbf{i}_{\mathbf{q}}^{*+} = B^{+}\mathbf{v}_{\perp}^{+} \quad ; \quad B^{+} = \frac{Q}{\left|\mathbf{v}^{+}\right|^{2}}. \tag{10}$$

Under unbalanced grid faults, the instantaneous reactive power delivered to the grid differs from Q because of the interaction between the injected positive-sequence current and negative-sequence component of the grid voltage, namely

$$q = \mathbf{v}_{\perp} \cdot \mathbf{i}_{\mathbf{q}}^{*} = \underbrace{\mathbf{v}_{\perp}^{+} \cdot \mathbf{i}_{\mathbf{q}}^{*}}_{Q} + \underbrace{\mathbf{v}_{\perp}^{-} \cdot \mathbf{i}_{\mathbf{q}}^{*}}_{\tilde{q}}. \tag{11}$$

Likewise, the instantaneous active power delivered by the *BPSC* control strategy during an unbalanced grid fault can by calculated as

$$p = \mathbf{v} \cdot \mathbf{i}_{\mathbf{q}}^{*} = \underbrace{\mathbf{v}^{+} \cdot \mathbf{i}_{\mathbf{q}}^{*}}_{0} + \underbrace{\mathbf{v}^{-} \cdot \mathbf{i}_{\mathbf{q}}^{*}}_{\tilde{p}}. \tag{12}$$

III. Maximum Peak Value of the Reactive Currents

A crucial issue in the control of a STATCOM during unbalanced transient faults is to guarantee that the peak value of the current injected into the grid by any of its three phases is always bellow of the maximum current limit. Otherwise, the STATCOM over-current protections will trip and consequences for the power system can become disastrous. In this section, mathematical expressions for calculating the maximum peak value of the current injected into the grid by the *PNSC*, *AARC* and *BPS* strategies are deduced.

A.- Peak current for the PNSC strategy

In (5), the value of $\mathbf{v}_{\perp}^{+} - \mathbf{v}_{\perp}^{-}$ in is given by:

$$\begin{aligned}\mathbf{v}_{\perp}^{+} - \mathbf{v}_{\perp}^{-} = \sqrt{\tfrac{3}{2}}\Big\{\big[-\hat{V}^{+}\sin(\theta+2\delta) - \hat{V}^{-}\sin(\theta)\big] + \\ j\big[\hat{V}^{+}\cos(\theta+2\delta) - \hat{V}^{-}\cos(\theta)\big]\Big\},\end{aligned} \tag{13}$$

where δ is defined as $\delta = \frac{1}{2}(\phi^{+} + \phi^{-})$.

In (13), it has been considered $\phi^{-} = 0$ without lack of generality of the analysis. Therefore, the $\alpha\beta$ components of the reference reactive current vector of (5) are given by:

$$\begin{aligned} i_{q\alpha}^{*} &= \Re\mathfrak{e}\big(\mathbf{i}_{q}^{*}\big) = \sqrt{\tfrac{2}{3}}\,Q\,\frac{-\hat{V}^{+}\sin(\theta+2\delta) - \hat{V}^{-}\sin(\theta)}{\hat{V}^{+^2} - \hat{V}^{-^2}}, \\ i_{q\beta}^{*} &= \Im\mathfrak{m}\big(\mathbf{i}_{q}^{*}\big) = \sqrt{\tfrac{2}{3}}\,Q\,\frac{\hat{V}^{+}\cos(\theta+2\delta) - \hat{V}^{-}\cos(\theta)}{\hat{V}^{+^2} - \hat{V}^{-^2}}. \end{aligned} \tag{14}$$

In the *PNSC* strategy, the maximum peak value of the current is given for the phase *a* when $-\pi/6 < \delta < \pi/6$. By using the *Clarke* transformation to pass from the $\alpha\beta$ to the *abc* domain, the current at the phase *a* is given by:

$$i_{a} = -\frac{2}{3}\,Q\,\frac{\hat{V}^{+}\sin(\theta+2\delta) + \hat{V}^{-}\sin(\theta)}{\hat{V}^{+^2} - \hat{V}^{-^2}}. \tag{15}$$

The i_a current presents its peak value for a θ_M phase-angle given by:

$$\theta_{M} = \arctan\left(\frac{\hat{V}^{+}\cos(2\delta) + \hat{V}^{-}}{\hat{V}^{+}\sin(2\delta)}\right). \tag{16}$$

Therefore, by substituting the phase-angle of (16) into (15) and simplifying, the maximum peak value of the current at the phase *a* is given by:

$$I_{M\delta} = \frac{2}{3}\,Q\,\frac{\sqrt{(\hat{V}^{+} - \hat{V}^{-})^{2} + 4\hat{V}^{+}\hat{V}^{-}\cos^{2}(\delta)}}{\hat{V}^{+^2} - \hat{V}^{-^2}}\Bigg|_{-\frac{\pi}{6}\le\delta\le\frac{\pi}{6}}. \tag{17}$$

In case that δ was out of the sector specified in (17), the maximum peak current would be given in the either phase *b* or *c*. However, the peak current could be still calculated by (17) after shifting δ by a multiple of $\pi/3$ until reaching the $\left[-\frac{\pi}{6},\frac{\pi}{6}\right]$ sector.

B.- Peak current for the AARC strategy

In (7), the value of $\mathbf{v}_{\perp} = \mathbf{v}_{\perp}^{+} + \mathbf{v}_{\perp}^{-}$ in is given by:

$$\begin{aligned}\mathbf{v}_{\perp}^{+} + \mathbf{v}_{\perp}^{-} = \sqrt{\tfrac{3}{2}}\Big\{\big[-\hat{V}^{+}\sin(\theta+2\delta) + \hat{V}^{-}\sin(\theta)\big] + \\ j\big[\hat{V}^{+}\cos(\theta+2\delta) + \hat{V}^{-}\cos(\theta)\big]\Big\}.\end{aligned} \tag{18}$$

Therefore, the $\alpha\beta$ components of the reference current vector calculated by (7) are given by:

$$\begin{aligned} i_{q\alpha}^{*} &= \Re\mathfrak{e}\big(\mathbf{i}_{q}^{*}\big) = \sqrt{\tfrac{3}{2}}\,Q\,\frac{-\hat{V}^{+}\sin(\theta+2\delta) + \hat{V}^{-}\sin(\theta)}{\hat{V}^{+^2} + \hat{V}^{-^2}} \\ &, \\ i_{q\alpha}^{*} &= \Im\mathfrak{m}\big(\mathbf{i}_{q}^{*}\big) = \sqrt{\tfrac{3}{2}}\,Q\,\frac{\hat{V}^{+}\cos(\theta+2\delta) + \hat{V}^{-}\cos(\theta)}{\hat{V}^{+^2} + \hat{V}^{-^2}} \end{aligned} \tag{19}$$

In the *AARC* strategy, the maximum peak value of the current is given for the phase *b* when $0 < \delta < \pi/3$. By using the *Clarke* transformation, the phase *b* current is given by:

$$\begin{aligned} i_{b} = \frac{2}{3}\,\frac{Q}{\hat{V}^{+^2} + \hat{V}^{-^2}}\big[\hat{V}^{+}\cos(\theta+2\delta+\tfrac{\pi}{6}) + \\ \hat{V}^{-}\cos(\theta-\tfrac{\pi}{6})\big]. \end{aligned} \tag{20}$$

The angle θ_M that leads to the maximum current in the (20) can by calculated by:

$$\theta_{M} = \arctan\left(\frac{\hat{V}^{+}\big[\cos(2\delta) - \sqrt{3}\sin(2\delta)\big] - \hat{V}^{-}}{\hat{V}^{+}\big[\sin(2\delta) + \sqrt{3}\cos(2\delta)\big] + \sqrt{3}\hat{V}^{-}}\right) \tag{21}$$

and the peak current can be calculated by just replacing (21) into (20), that is:

$$I_{M\delta} = i_{b}(\theta_{M}). \tag{22}$$

C.- Peak current for the BPSC strategy

In the *BPSC* strategy, the amplitude of the current vector is constant. Therefore, the three phase currents are sinusoidal and balanced, with a peak value that can be calculated by:

$$I_{M\delta} = \frac{2}{3}\frac{Q}{\hat{V}^+}. \tag{23}$$

D.- Discussion

Expressions of (17), (22) and (23) allow calculating the maximum current in any of the phases of the STATCOM when it is delivering a given reactive power Q under certain unbalanced grid conditions characterized by $\hat{V}^+$, $\hat{V}^-$ and δ. In a practical case however, it is more interesting to use the expressions shown in (24), (25) and (26) to determine the highest reactive power that can be injected by the STATCOM (Q_M) in an unbalanced grid scenario without tripping the over-current protection of any of its phases, i.e., the phase currents will keep always bellow a given current limit I_{lim}.

PNSC:

$$Q_M = \frac{3}{2}\frac{I_{\text{lim}}\left(\hat{V}^{+^2} - \hat{V}^{-^2}\right)}{\sqrt{(\hat{V}^+ - \hat{V}^-)^2 + 4\hat{V}^+\hat{V}^-\cos^2(\delta)}} \tag{24}$$

AARC:

$$Q_M = \frac{3}{2}\frac{I_{\text{lim}}\left(\hat{V}^{+^2} + \hat{V}^{-^2}\right)}{\hat{V}^+\cos(\theta_M + 2\delta + \frac{\pi}{6}) + \hat{V}^-\cos(\theta_M - \frac{\pi}{6})} \tag{25}$$

BPSC:

$$Q_M = \frac{3}{2} I_{lim}\hat{V}^+ \tag{26}$$

IV. Simulation Results

To validate the expressions obtained from the study conducted in §III, some simulations were performed by using the software PSCAD/EMTDC. The algorithm to calculate the reference currents was implemented on the natural *abc* reference frame, so the orthogonal voltage vector was calculated by:

$$\mathbf{v}_\perp = \left[T_\perp\right]\mathbf{v}_{abc}; \qquad \left[T_\perp\right] = \frac{1}{\sqrt{3}}\begin{bmatrix} 0 & -1 & 1 \\ 1 & 0 & -1 \\ -1 & 1 & 0 \end{bmatrix}. \tag{27}$$

A FLL based on a second-order generalized integrator (SOGI) [S] was used in these simulations to detect the parameters of the positive- and negative-sequence components of the unbalanced grid voltage during asymmetrical faults. In the FLL, the angle δ is calculated as:

$$\delta = \frac{1}{2}\cos^{-1}\left(\frac{\mathbf{v}^+_{\alpha\beta}\cdot\mathbf{v}^{-(*)}_{\alpha\beta}}{\hat{V}^+\hat{V}^-}\right). \tag{28}$$

where $\mathbf{v}^+_{\alpha\beta}$ and $\mathbf{v}^-_{\alpha\beta}$ are the positive- and negative-sequence voltage vectors on $\alpha\beta$ reference frame, respectively, and the superscript (*) denotes the complex conjugate operator.

In the simulation case considered in this section, the STATCOM injected zero reactive current into the grid during the prefault period (Q^*=0) and, once the grid fault is detected, it injected the highest allowed reactive power (Q^*=Q_M) without overpassing a current limit (I_{lim}), which was set as a reference input in the simulation model. Fig. 2 shows a simplified diagram of the control structure used in these simulations. A fault detector is used to change the reactive power reference when a fault occurs.

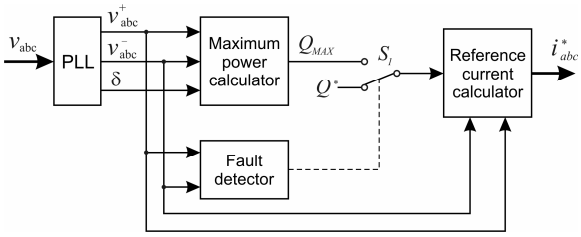

Fig. 2 Simplified diagram of the STATCOM control structure.

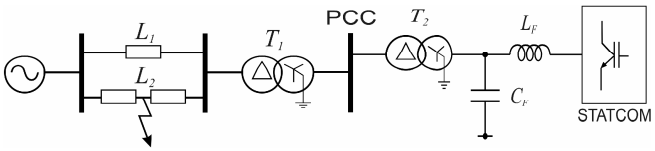

Fig. 3 Electrical scheme of the wind power plant considered in simulation.

In simulation, the STATCOM was connected to ac collector of a wind power plant (WPP) through a 33kV/690V transformer (T_2). The WPP connects to the electrical system through a second 120kV/33kV transformer (T_1). The connection of the WPP was represented by two parallel lines (L_1//L_2).

To test the effectiveness of the proposed reactive current control strategies, a line-to-ground fault was considered at the half of L_2, which resulted in a type B dip propagated to the y winding of T_1 as a type C dip and to the y winding of T_2 as a type D dip [16]. The positive- and negative-sequence voltage phasors during the fault were given by $\mathbf{V}^+ = 0.84\underline{|0^o}$ and $\mathbf{V}^- = 0.16\underline{|58^o}$, being the pre-fault voltage $V^+_{pf} = 1\underline{|0^o}$ p.u.. The rated power of the simulated STATCOM was 10Mvar, being its rated current 8.367 kA. Therefore, the current limit was set to I_{lim} = 11.833 kA ($\sqrt{2}$ 8.367). The simulation results are shown in Fig. 3 for each control strategy. Note that none of the currents overpasses the current limit I_{lim} (shown in Fig 4 by a dot line) in any time.

The simulation results of Fig. 4 demonstrate how the current limiting expressions found in §III where able to keep the phase currents below the current limit for the three proposed control strategies, even when the grid voltage is highly unbalanced. It is possible to appreciate in these plots how, after a transient period needed by the FLL to detect the grid fault parameters, the injected reactive currents are perfectly sinusoidal for all the three proposed strategies. In these simulations, the phase currents transitorily overpass the current limit during very short periods, even though the injected current is under control in steady state conditions.

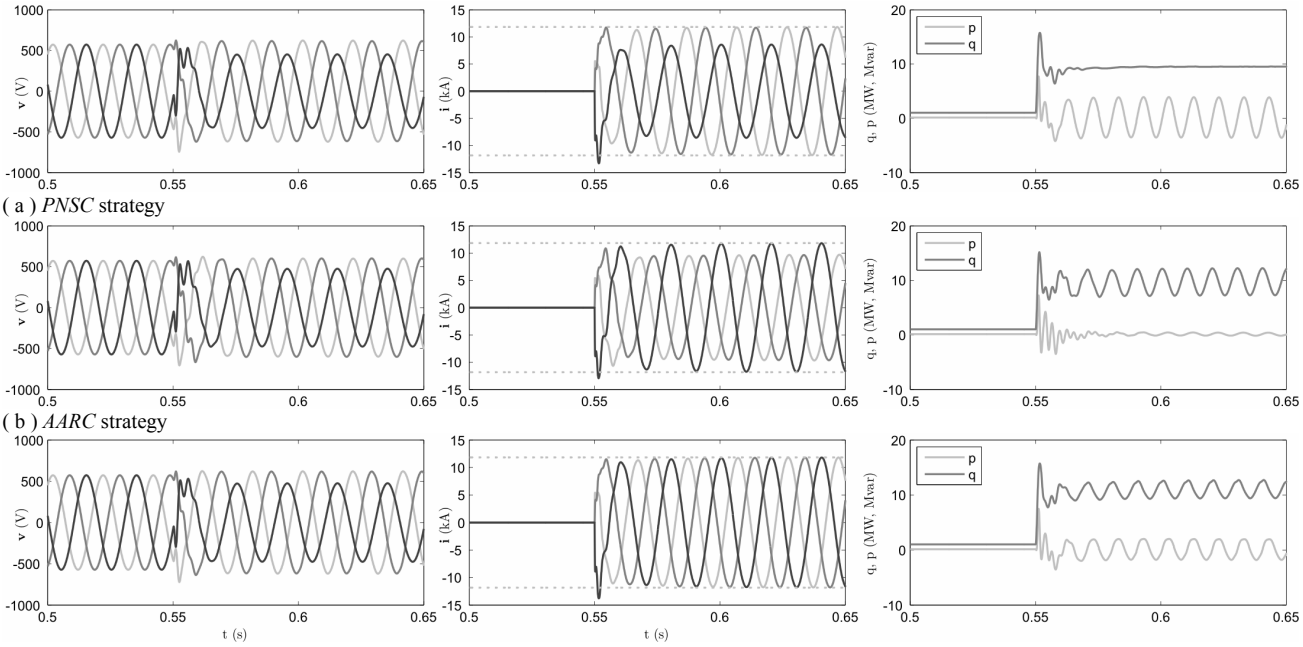

(a) *PNSC* strategy

(b) *AARC* strategy

(c) *BPSC* strategy

Fig. 4 – Simulation results. Columns from left to right: grid voltage, injected currents and the converter current limit, instantaneous active and reactive power delivered to the grid.

It is due to the high dynamics set to the STATCOM controller and the small link filter used in simulation. As proven later by experimental results, these short over-currents did not exist when the STATCOM presented a slower dynamic respzonse. Plots representing instantaneous powers in Fig. 4 corroborate that the *PNSC* strategy cancels any oscillation in the injected reactive power resulting from the interaction of voltages and currents with different sequences. However, as expected from (6), this strategy gives rise to oscillations in the delivered instantaneous active power, which implies oscillations in the dc-bus voltage. The *AARC* strategy does not generate dc-bus voltage oscillations since it does not deliver any active power. However, the injected reactive power presents some oscillations. In the case of the *BPSC* strategy, the injected currents are perfectly sinusoidal with positive sequence during the grid fault, which gives rise to oscillations in both the active and reactive power.

V. Experimental Results

The proposed reactive current control strategies were evaluated in an experimental setup shown in Fig. 5. The STATCOM was connected to the grid through a Δy transformer. The STATCOM consisted of a current-controlled VSI and a LC link filter connected. The grid consisted of another transformer with several taps. In the experiments, the grid fault was simulated by switching between two taps of the grid transformer, which gave rise to a voltage sag of 50% on phase *c*. This single-phase fault (type B dip) was propagated to the y winding of the transformer as a type C dip [B]. A dSpace 1103 DSP card was used to implement the reactive current injection strategies, the current limiter controller, the FLL and the low level resonant current controllers. The sampling and the switching frequencies in the experiments were set to 10 kHz and 20 kHz, respectively.

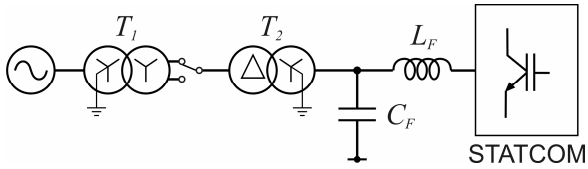

Fig. 5 Experimental setup used for testing the proposed control strategies.

In the experimental results shown in this section, in contrast to the simulations of §IV, the STATCOM was injected the maximum level of reactive current during the prefault period. The current limit for the STATCOM in these experiments was set to 5A.

Figures 6(a), 6(b) and 6(c) show the grid voltages and the currents injected by the STATCOM for each control strategy. In these figures, the current scale is of 1A/V. Figures 6(d), 6(e) and 6(f) show the instantaneous active and reactive powers associated to previous voltage and currents waveforms.

It can be appreciated in Figures 6(a), 6(b) and 6(c) the excellent performance of the proposed control strategies. The reactive currents injected by the experimental STATCOM do not overpass the current limit in any time, even when the operating conditions were very severe, since the STATCOM was working at its maximum operating limit before the grid fault.

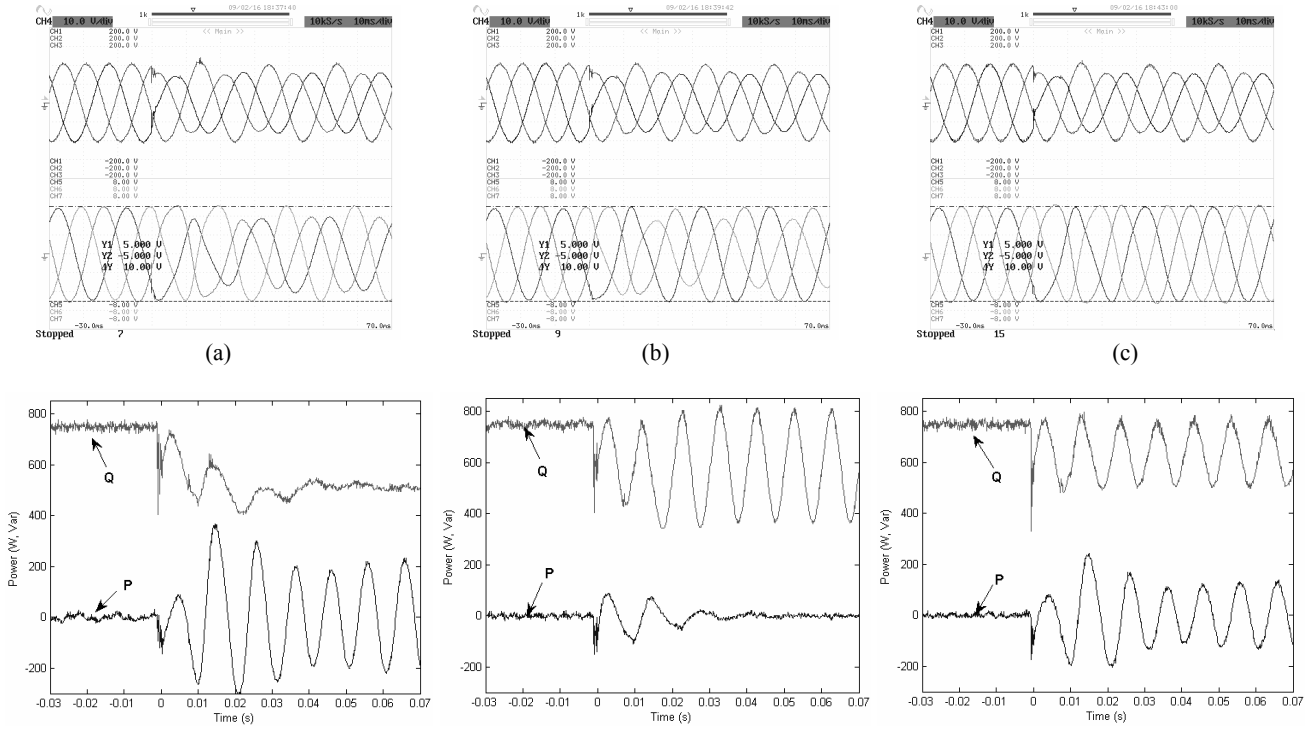

Fig. 6 Experimental results. (a) Grid voltages and currents for PNSC, (d) Active and reactive power for PNSC, (b) Grid voltages and currents for AARC, (e) Active and reactive power for AARC, (c) Grid voltages and currents for BPSC, (f) Active and reactive power for BPSC.

The dynamics of the experimental STATCOM is slightly slower that the one considered in simulation. This fact can be appreciated in Figures 6(d), 6(e) and 6(f), where the instantaneous power presents a longer settle time before reaching steady state conditions during the grid fault.

It is worth to remark the excellent performance of the FLL, which is able to detect the new grid conditions during the faults in around one grid cycle. It is also necessary to highlight the good performance of the resonant controllers used in the experimental setup, which allow injecting very high quality currents into the grid and give rise to instantaneous powers perfectly matching the waveforms obtained in simulation.

VI. Conclusion

This paper presented three reactive current control strategies to achieve an effective and safe operation of a STATCOM during unbalanced grid faults.

The algorithms for calculating the reference currents in the proposed control strategies were deduced by using a generic space vector approach and the different terms in the reactive power injected into the grid were properly identified.

An exhaustive analysis of the current vector locus for each of the proposed strategies allowed deducing mathematical expressions for calculating the maximum peak value of the current injected into the grid by the STATCOM as a function of the unbalanced grid conditions and the reactive power level. This analysis allowed determining the maximum reactive power that can be delivered into the grid under particular unbalanced grid conditions to do not overpass in any of the STATCOM phases a current limit set as a reference input.

The proposed control strategies were implemented in simulation to control a STATCOM operating in a WPP by using PSCAD/EMTDC. Unbalanced faults were generated in the lines connecting the WPP. The results obtained from these simulations validated the effectiveness of the mathematical expression to control the STATCOM in a safe mode under unbalanced grid conditions.

The proposed reactive current control strategies were also evaluated by using an experimental setup. Different grid faults were simulated in the lab. The experimental results corroborated the excellent performance of the STATCOM operating under unbalanced grid conditions when controlled by the control strategies presented in this paper.

Acknowledgment

This work was supported by the project ENE2008-06841-C02-01/ALT. The authors would like to recognize the support of CAPES and CNPq.

REFERENCES

[1] E. Acha, V. Agelidis, O. Anaya-Lara and T.J. Miller, "Power Electronics Control in Electrical Systems", Newnes, 2002, ISBN 0-7506-5126-1.

[2] L. Gyugyi, "Dynamic compensation of AC transmission lines by solid-state synchronous voltage sources," *IEEE Trans. on Power Delivery*, vol.9, no.2, pp.904-911, Apr 1994

[3] L.Kuang, L. Jinjun, W. Zhaoan, W. Biao, "Strategies and Operating Point Optimization of STATCOM Control for Voltage Unbalance Mitigation in Three-Phase Three-Wire Systems," *IEEE Trans. on Power Delivery*, vol.22, no.1, pp.413-422, Jan. 2007.

[4] A. Edris, "FACTS technology development: an update," *IEEE Power Engineering Review*, vol.20, no.3, pp.4-9, Mar 2000.

[5] C. Han; Z. Yang, B. Chen, A.Q. Huang, Z. B. Zhang, M.R. Ingram, A.-A. Edris, "Evaluation of Cascade-Multilevel-Converter-Based STATCOM for Arc Furnace Flicker Mitigation," *IEEE Tran. on Ind. Applicat.*, vol.43, no.2, pp.378-385, March-april 2007.

[6] A. Jain, K. Joshi, A. Behal, N. Mohan, "Voltage regulation with STATCOMs: modeling, control and results," *IEEE Trans. On Power Delivery*, vol.21, no.2, pp. 726-735, April 2006.

[7] C. Han, A.Q. Huang, M.E. Baran, S. Bhattacharya, W. Litzenberger, L. Anderson, A.L. Johnson, A.-A. Edris, "STATCOM Impact Study on the Integration of a Large Wind Farm into a Weak Loop Power System," *IEEE Trans. on Energy Conversion*, vol.23, no.1, pp.226-233, March 2008

[8] "Grid Code. High and extra high voltage", E.ON Netz GmbH, Germany, Apr. 2006.

[9] "Grid connection of wind turbines to networks with voltages above/below 100 kV", Energinet, regulations TF 3.2.5/TF 3.2.6, Denmark, Dec. 2004/May 2004.

[10] "Response requirements for electricity production facilities under special regulation in the presence of voltage sags,"(in Spanish), REE, PO 12.3, Spain, Oct. 2006.

[11] M. Molinas, J. Are; T. Undeland, "Low Voltage Ride Through of Wind Farms With Cage Generators: STATCOM Versus SVC," *IEEE Trans. on Power Electronics*, vol.23, no.3, pp.1104-1117, May 2008

[12] S. Mori, K. Matsuno, T. Hasegawa, S. Ohnishi, M. Takeda, M. Seto, S. Murakami, F. Ishiguro, "Development of a large static VAr generator using self-commutated inverters for improving power system stability," *IEEE Trans. on Power Systems*, vol.8, no.1, pp.371-377, Feb 1993

[13] C. Hochgraf, R.H. Lasseter, "Statcom controls for operation with unbalanced voltages," *IEEE Trans. on Power Delivery*, vol.13, no.2, pp.538-544, Apr 1998.

[14] K. Li, J. Liu, Z. Wang, B. Wei, "Strategies and operating point optimization of STATCOM control for voltage unbalance mitigation in three-phase three-wire systems," *IEEE Trans. on Power Delivery*, vol.22, no.1, pp.413-422, Jan 2007.

[15] P. Rodriguez, A.V. Timbus, R. Teodorescu, M. Liserre, and F. Blaabjerg, "Reactive power control for improving wind turbine system behaviour under grid faults," *IEEE Trans. on Power Electronics*, to be published in 2009.

[16] M.H.J. Bollen and L.D. Zhang, "Different methods for classification of three-phase unbalanced voltage dips due to faults," *Electric Power Systems Research*, vol. 66, num. 1, pp. 59-69, July 2003.